LCnote LC-PHSM-2005-001

Determination of beam energy at TESLA using radiative return events

ARND HINZE

DESY Zeuthen
Platanenallee 6, 15738 Zeuthen, Germany, EU

Radiative return events can be used to determine the beam energy at TESLA. It was suggested to use this method to cross check and calibrate the magnet spectrometer used for measurement of the beam energy at TESLA. A preliminary assessment of the statistical and systematic errors of this method is performed here.

Contents

I. Introduction

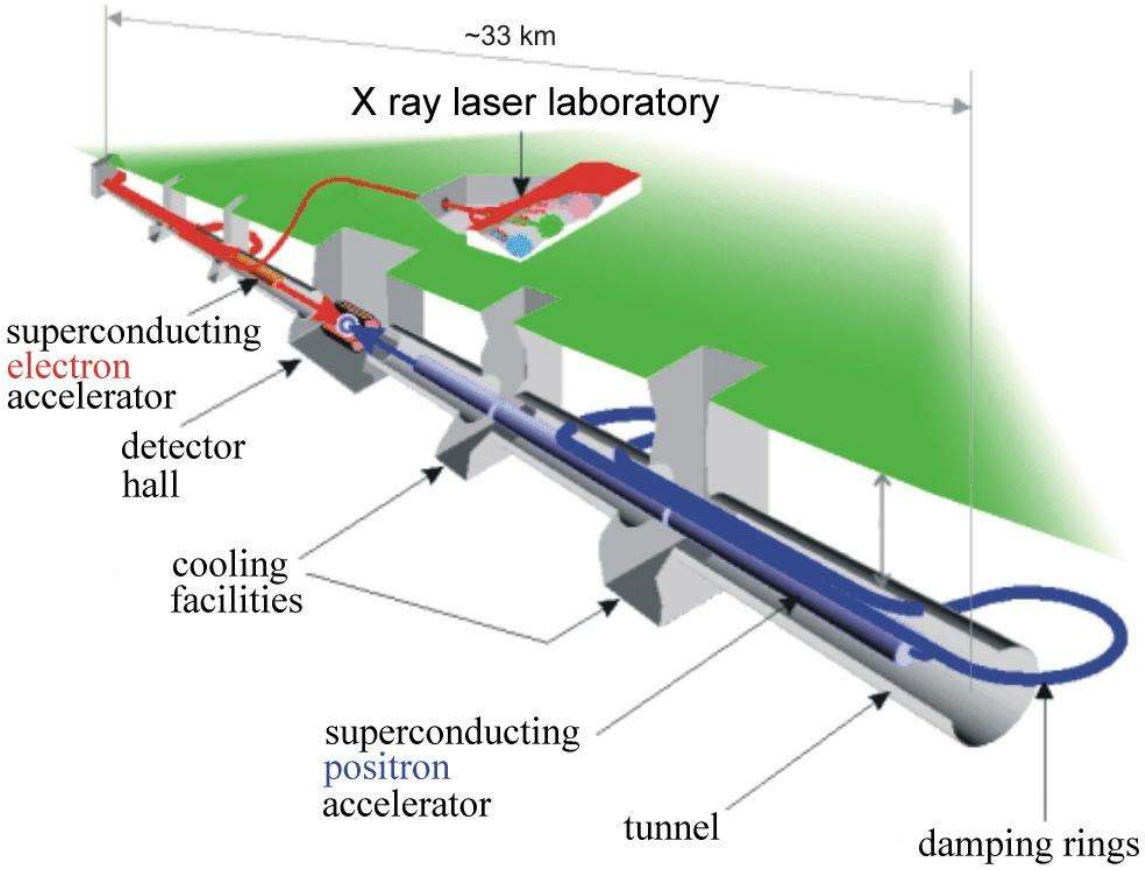

Fig 1: S*chematic view of TESLA*

TESLA stands for **T**era electron volt **E**nergy **S**uperconducting **L**inear **A**ccelerator. TESLA is the superconducting version of the next linear accelerator planned. It has been developed so far in international collaboration at DESY. After the TESLA technology has now been recommended for the next linear accelerator the development moves under the joint ILC (**I**nternational **L**inear **C**ollider) Project.
In fig. 1 you see a schematic view of TESLA [1]. It consists of one part to accelerate electrons, one part to accelerate positrons and the detector at the center. The superconducting cavities for acceleration are build into a tunnel which has in certain distances cooling facilities installed. In the damping rings the diameter and the divergence of the electron and positron beams are reduced. A large diameter and high divergence would reduce the interaction rate of the electron and the positron beam.
The x ray laser laboratory is an additional project in development at DESY.

TESLA will have a center of mass energy of about 500 GeV which can be expanded to 1 TeV. It will have a luminosity above $3.4*10^{34}$ cm^{-2} s^{-1} which corresponds to an integrated luminosity of 340 fb^{-1} for a year (i.e. 10^7 s). The length will be about 33 km and TESLA will operate at a temperature of 2 K consuming about 100 MW power. The electrons will be generated in a polarised laser driven gun [1]. One option to produce the positrons is to pass the already preaccelerated polarized electron beam of an energy of 150 GeV through a helical undulator. Circularly polarized photons of about 11 MeV are generated and the electron beam is further accelerated and brought to the interaction point. The circularly polarized photons are converted to electron positron pairs in a thin target. The polarization of the photons is transferred to the polarization of the electron/positron pairs and the polarized positrons are captured behind the target to form a positron beam which is then fed into the accelerator. Through this method a polarization of 80% of the electron beam and of 60% of the positron beam can be achieved [11]. The beams are actually not continuous but come in bunches with 337 ns pause in between.
TESLA will allow to further test the Standard Model. It is important for the search of the Higgs particle and may give new hints for physics beyond the Standard Model. For example it may be possible to verify Supersymmetry or at least draw borders on Supersymmetry parameters.

For high precision measurements at the linear collider TESLA, for example the measurement of the higgs mass, top quark mass or W mass, a precise knowledge of the beam energy is essential. To achieve this it was proposed to use a magnet spectrometer positioned upstream of the interaction point (IP), see also [1] and [5]. To cross check and calibrate this device it was suggested to utilize an independent method that uses radiative return events, i. e. events where the e^+e^- annihilate to produce a particle – antiparticle pair and a photon, whose emission "returns" the center of mass energy of the pair to the Z^0 peak.
The knowledge of the precision of this method is important for the planning of experiments and the design of the magnet spectrometer to achieve high precision in energy regions of interest.
In this study Monte Carlo simulations are performed to determine the precision of the method.
In chapter II the method is introduced, chapter III treats the creation of the basic Monte Carlo sample and the statistical error. Chapter IV looks at the behavior of the statistical error of the method at different center of mass energies. In chapter V and VI the systematic errors of the method are treated. In chapter VII you find an overview of the major results.

II. The Method

1. General

Using relativistic kinematics (see chapter II. part 2.) it is possible to calculate the center of mass energy of a three body system using only the center of mass energy of two of the particles and the angles they make with the third particle (for example see fig. 3). One can apply this to processes at TESLA which have a three body final state to calculate the center of mass energy of the e^+e^- accelerated in TESLA. The calculated center of mass energy can then be used to calibrate the detector of beam energy at TESLA (a magnet spectrometer: see[1], [5]).

The energies and angles of the particles produced in these processes have to be measured by a detector. But the calibration of the magnet spectrometer and calibration of the energy determination of the particle detector are correlated. To circumvent this correlation one first wants to calibrate the magnet spectrometer without measuring particle energies. To make the calculation of the center of mass energy independent of energy measurements, one takes only processes going over an intermediate Z^0 state. The Z^0 mass is known precisely and since the Z^0 decays into particle-antiparticle pairs its mass can be used as the center of mass energy of the pair.

Of the processes with an intermediate Z^0 the one with the least background is $e^+e^- \rightarrow Z^0/\gamma^* \rightarrow \mu^+\mu^-\gamma$, since it is possible to discern between muons and electrons / positrons, in case of background where electrons or positrons are in the final state (See also [2]). In addition the muon lifetime guarantees easy reconstruction of the process in the particle detector.

Monte Carlo samples are created to simulate experimental data samples which will be measured at TESLA. A fit is performed on these samples to get an estimation of the statistical errors the method will have for real data samples from TESLA. The samples are also used to study systematic errors of the method.

$\Delta\sqrt{s}/\sqrt{s}=\Delta E_{beam}/E_{beam}$ should be smaller than 10^{-4} to avoid dominating the expected errors in the determination of top quark mass and higgs mass by the uncertainty in the determination of the beam energy [5]. At 350 GeV center of mass energy it follows that $\Delta\sqrt{s}=2\Delta E_{beam}$ should be smaller than 35 MeV.

2. Kinematics

In the following c=1.
The process considered in this study is (see fig. 2):

$$e^+e^- \rightarrow Z^0/\gamma^* \rightarrow \mu^+\mu^-\gamma$$

For three body systems one can calculate the energy of the system using the angles of two of the bodies with respect to the third.
Thus if exactly one photon is radiated the invariant energy of the system can be calculated using the angles of the muons w. r. t. the direction in which the photon is emitted.

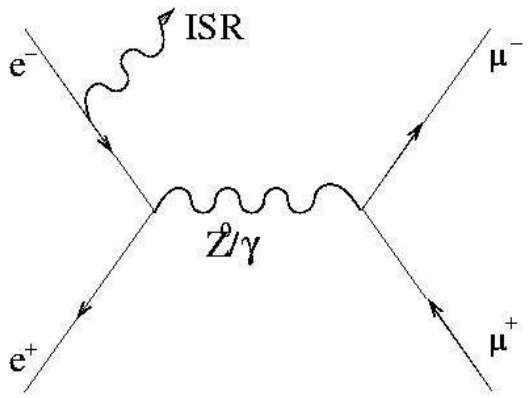

Fig. 2: *The process* $e^+e^- \rightarrow Z^0/\gamma^* \rightarrow \mu^+\mu^-\gamma$

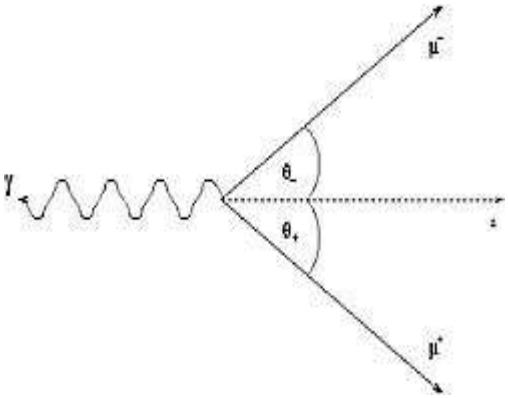

Fig. 3: *The final three body system*

For the three momenta in fig. 3 the following relation holds:

$$\mathbf{p}_{\mu-} + \mathbf{p}_{\mu+} + \mathbf{p}_{\gamma} = 0 \tag{1}$$

thus:

$$|\mathbf{p}_{\mu-}|\sin(\theta_-) - |\mathbf{p}_{\mu+}|\sin(\theta_+) = 0 \tag{2}$$

$$|\mathbf{p}_{\mu-}|\cos(\theta_-) - |\mathbf{p}_{\mu+}|\cos(\theta_+) - |\mathbf{p}_{\gamma}| = 0 \tag{3}$$

the invariant energy is defined as:

$$\sqrt{s} = \sqrt{(E_{\mu-} + E_{\mu+} + E_{\gamma})^2 - (\mathbf{p}_{\mu-} + \mathbf{p}_{\mu+} + \mathbf{p}_{\gamma})^2}$$

neglecting the muon mass (≈ 0.1 GeV) and using (1) in the formula for the invariant energy:

$$\sqrt{s} \approx |\mathbf{p}_{\mu-}|+|\mathbf{p}_{\mu+}|+|\mathbf{p}_{\gamma}| \tag{4}$$

use (2) in (4) to substitute for $|\mathbf{p}_{\mu+}|$:

$$|\mathbf{p}_{\mu-}| = \frac{\sqrt{s}-|\mathbf{p}_{\gamma}|}{1+\frac{\sin(\theta_-)}{\sin(\theta_+)}}$$

insert this in (3) to substitute for $|\mathbf{p}_{\mu-}|$:

$$0 = \frac{\sqrt{s}-|\mathbf{p}_{\gamma}|}{1+\frac{\sin(\theta_-)}{\sin(\theta_+)}}(\cos(\theta_-)+\frac{\sin(\theta_-)}{\sin(\theta_+)}\cos(\theta_+))-|\mathbf{p}_{\gamma}| \tag{5}$$

solve for $|\mathbf{p}_{\gamma}|$:

$$|\mathbf{p}_{\gamma}| = \sqrt{s}\frac{\sin(\theta_+)\cos(\theta_-)+\sin(\theta_-)\cos(\theta_+)}{\sin(\theta_+)+\sin(\theta_-)+\sin(\theta_+)\cos(\theta_-)+\sin(\theta_-)\cos(\theta_+)}$$

$$= E_{\gamma}$$

define κ_{γ}:

$$\kappa_{\gamma} := \frac{E_{\gamma}}{\frac{1}{2}\sqrt{s}} = 2\frac{\sin(\theta_+)\cos(\theta_-)+\sin(\theta_-)\cos(\theta_+)}{\sin(\theta_+)+\sin(\theta_-)+\sin(\theta_+)\cos(\theta_-)+\sin(\theta_-)\cos(\theta_+)}$$

(6)

Now use $s' = (p_{\mu-} + p_{\mu+})^2$, $s = (p_{\mu-} + p_{\mu+} + p_\gamma)^2$ and conservation of four momentum $p_{\varepsilon-} + p_{\varepsilon+} = p_{\mu-} + p_{\mu+} + p_\gamma$:

$$\sqrt{s'} = \sqrt{(p_{\mu-} + p_{\mu+})^2} = \sqrt{(p_{e-} + p_{e+} - p_\gamma)^2}$$

$$= \sqrt{(p_{e-} + p_{e+})^2 + p_\gamma^2 - 2\,p_\gamma (p_{e-} + p_{e+})}$$

use $p_\gamma^2 = m_\gamma = 0$, $s = (p_{e-} + p_{e+})^2$:

$$= \sqrt{s - 2E_\gamma (E_{e-} + E_{e+}) - \mathbf{p}_\gamma (\mathbf{p}_{e-} + \mathbf{p}_{e+})}$$

use $\sqrt{s} = E_{e-} + E_{e+}$, $\mathbf{p}_{e-} + \mathbf{p}_{e+} = 0$:

$$\sqrt{s'} = \sqrt{s - 2E_\gamma \sqrt{s}} \tag{7}$$

use definition (6):

$$\sqrt{s'} = \sqrt{s - \kappa_\gamma s}$$

$$\sqrt{s'} = \sqrt{s}\sqrt{1 - \kappa_\gamma} \tag{8}$$

In the present study we do not want to use the muon energy, but only the angles the muons make with the emitted photon. If we use only events where the invariant energy of the two muons is near the Z mass peak, we can set $\sqrt{s'} \approx m_Z$:

$$\sqrt{s} \approx \frac{m_Z}{\sqrt{1 - \kappa_\gamma}} \tag{9}$$

This formula is used in the following to calculate the invariant mass of the $\mu^+\mu^-\gamma$ system from the angles of the muons. The whole angular dependence lies in the factor κ_γ.

If the muon masses are taken into account one arrives at:

$$|\mathbf{p}_\gamma| = \frac{\sqrt{s}-|\mathbf{p}_\gamma|}{1+\frac{1}{x}}(\cos(\theta_-)+\frac{1}{x}\cos(\theta_+)) \quad *$$

$$\sqrt{\frac{1}{(x-1)^2}(x^2+1-\sqrt{4x^2+\frac{4(x^2-1)^2}{(\sqrt{s}-|\mathbf{p}_\gamma|)^2}m_\mu^2})}$$

$$= E_\gamma \tag{10}$$

where $x=\frac{\sin(\theta_+)}{\sin(\theta_-)}$. If m_μ is set 0 the root reduces to 1 and one arrives at (5).
Now using (7) in the form:

$$E_\gamma = \frac{s-s'}{2\sqrt{s}}$$

using $|\mathbf{p}_\gamma| = E_\gamma$ and inserting into (10):

$$\frac{s-s'}{2\sqrt{s}} = \frac{\sqrt{s}-\frac{s-s'}{2\sqrt{s}}}{1+\frac{1}{x}}(\cos(\theta_-)+\cos(\theta_+)) \quad *$$

$$\sqrt{\frac{1}{(x-1)^2}(x^2+1-\sqrt{4x^2+\frac{4(x^2-1)^2}{(\sqrt{s}-\frac{s-s'}{2\sqrt{s}})^2}m_\mu^2})}$$

(11)

one arrives at a formula for s and s' which can be solved numerically, should the influence of the masses become important. This is the case for particles of very high masses as the τ and the top quark.

3. Fit method

For the Monte Carlo samples created in this study it is difficult to find simple, yet well fitting functions. Because of this another method was adopted, namely to use two Monte Carlo samples to fit a third one. One creates two Monte Carlo samples generated at only slightly different center of mass energies. A large number of events is generated to get small statistical fluctuations in these samples. Furthermore one needs some experimental data sample or as in this case one creates a third Monte Carlo sample to simulate the experimental data.

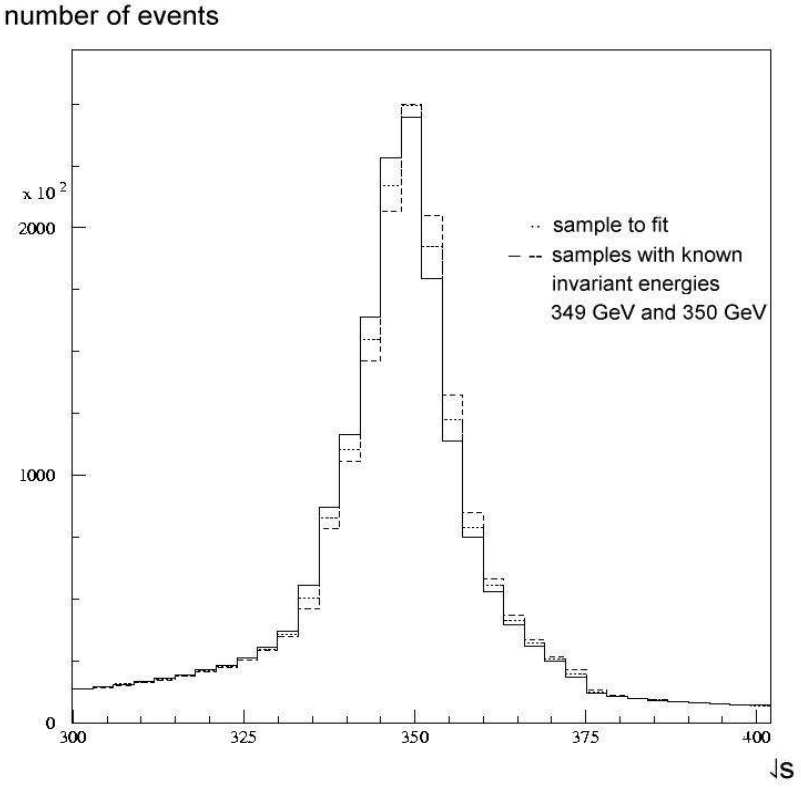

Fig. 4: *Two Monte Carlo samples to fit a third one*

The fit method makes the assumption of a linear relationship between samples "near" each other in terms of the parameter in question. It corresponds to a Taylor expansion (see fig. 4):

$$N_i(x) = N_i(x_0) + \frac{N_i(x_1) - N_i(x_0)}{x_1 - x_0}(x - x_0) + \ldots \qquad (12)$$

Where $N_i(x)$ is the number of events in bin i of the experimental data, $N_i(x_0)$ the number of events of a Monte Carlo sample with known parameter x_0, $N_i(x_1)$ the number of events of another Monte Carlo sample with known parameter x_1.

Neglecting higher order terms, one minimizes the squared difference between the linear approximation and the data N(x), thus obtaining an estimate for the parameter x:

$$\chi^2 = \Sigma_{\text{bins}} \left(N_i(x) - \left(N_i(x_0) + \frac{N_i(x_1) - N_i(x_0)}{x_1 - x_0} (x - x_0) \right) \right)^2 \qquad (13)$$

The sum is over all bins of the histogram. In this study the parameter to be fitted is the invariant energy $\sqrt{s}$ of the $\mu^+\mu^-\gamma$ system, thus:

$$\chi^2 = \Sigma_{\text{bins}} \left(N_i(\sqrt{s}) - \left(N_i(\sqrt{s_0}) + \frac{N_i(\sqrt{s_1}) - N_i(\sqrt{s_0})}{\sqrt{s_1} - \sqrt{s_0}} (\sqrt{s} - \sqrt{s_0}) \right) \right)^2 \qquad (14)$$

Since the shape of the fitting function is provided by the data samples themselves, this method is especially suited for fitting data with difficult shapes, or where the parameter in question is not connected to any obvious property of the data shape like the position of a peak or the width of a peak etc. The method has to be tested whether the linearity assumption really holds. For example by fitting samples at different parameter values between x_1 and x_0 and looking whether they have the same shift and errors.

4. Complications to be simulated

There are several complications arising from the design of TESLA for determining the beam energy using radiative return events:

1.
In the coherent fields of the positron bunch the electrons start to radiate - and the positrons in the fields of the electron bunch. This is called beamstrahlung which is simulated in this study by means of the package CIRCE [10], which uses parameters derived by fitting extensive simulations of beamstrahlung. Beamstrahlung is build into the Monte Carlo simulation in chapter III part 3. Since the parameters are obtained through a fit procedure they have errors [4]. The resulting systematic errors are treated in chapter VI part 4.

2.
Not single electrons / positrons are accelerated but whole bunches and bunch trains. The particles in the bunch follow an energy distribution around the nominal beam energy. Simulations of TESLA suggest that this distribution will be gaussian [1]. The energy distribution is implemented in chapter III part 9. Chapter VI part 1 and 2 study the systematic errors induced by uncertainities in the distribution.

3.
The detector of TESLA can not detect particles below 3 degree from the accelerator axis, because the beam is passing there. Between 3° and 7° there is only space to install a calorimeter. Therefore one cannot distinguish charges, in particular electrons / positrons and photons, below 7° [1]. In addition it is not possible to reconstruct jet events below 7°. This is taken into account in chapter III part 4 and part 7.

4.
The aspect ratio of the detector (ratio between length in accelerator direction and transverse to it) will have a small uncertainty. This has been the source for a big shift in invariant energy at LEP [2]. Treated in chapter VI part 3.

5.
There are several background processes which can not be separated from the signal. This is treated in chapter III part 5, part 6 and part 7, furthermore in the whole chapter V.

III. Monte Carlo sample creation

A Monte Carlo sample has to be created which takes into account several complications like background, detector limitations and uncertainties in the energy of the particles.
In each of the following steps one additional complication is added to the Monte Carlo sample. In addition a fit of the Monte Carlo samples is performed in each step. This allows to track the behavior of the statistical error. Changes in the statistical error can then be assigned to the added complication.
The final sample then simulates hopefully closely the real data that will be measured at TESLA. It allows an estimation of the statistical error of the method and it can be applied to study the systematic errors of the method.
The first chapter introduces the concept of luminosity.

1. Concept of luminosity

Luminosity is the number of incident particles interacting with each other per area and time. For two colliding beams of same number of particles per bunch N it is given by the formula:

$$L = \frac{N^2 f}{4\pi\sigma_x\sigma_y} \tag{15}$$

Where f is the frequency of bunches, σ_x , σ_y are the transverse dimensions of the beam. $\pi\sigma_x\sigma_y$ is the area of the beam.

Integrated luminosity is the luminosity integrated over a certain time. For specifying the integrated luminosity of an accelerator usually a year is taken while it is assumed that the accelerator actually runs about 30% of the time.

Luminosity is used to express a number of events in terms of running time of the accelerator. To convert the number of events of a certain process to luminosity the cross section of the process is needed:

$$\sigma \int_0^t L\,dt = N \tag{16}$$

Where σ is the cross section of the process, L is the luminosity and N is the number of events of the process up to time t. Equation (16) can also be thought of as definition of luminosity.

2. Ideal beam:

As a first step only the annihilation of a positron and an electron into a Z^0 or excited photon and the subsequent decay into a muon-antimuon pair was simulated using PYTHIA [9]. The annihilation was simulated at a center of mass energy √s of 350 GeV. Fig. (5) shows a typical spectrum of the center of mass energy of the two muons √s'. The rest energy is emitted through a photon.
The Z^0 mass peak at 91 GeV and a peak at 350 GeV (only low energy photons emitted) are easy to see:

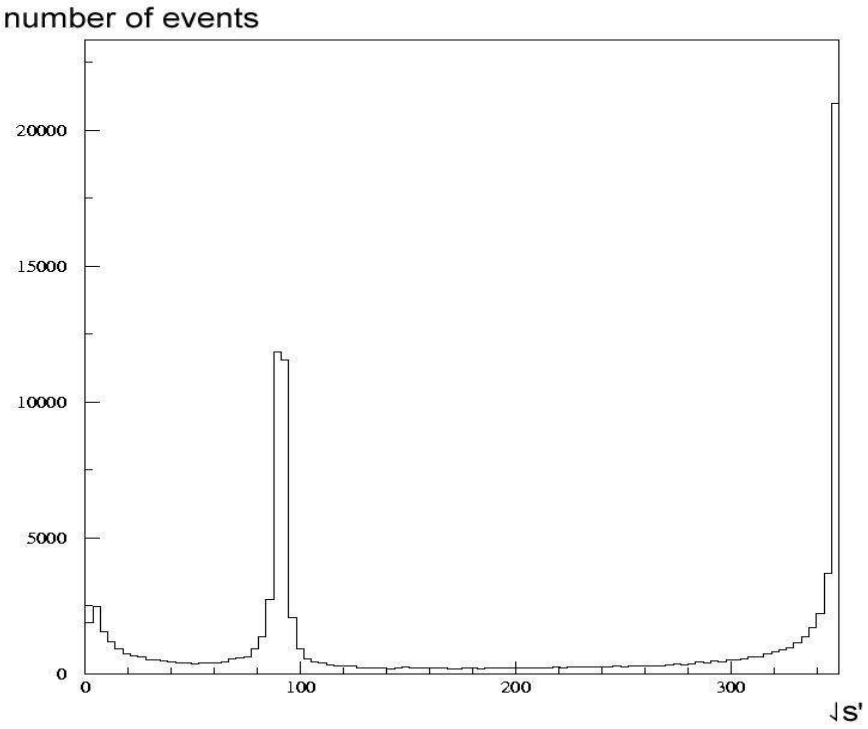

Fig. 5: *Invariant energy √s' of the two muons after the process*

Now equation (8) of Chapter II part 2 is applied. To use this equation we need the angles the muons make with the emitted photon and their center of mass energy √s' .
One arrives at the following ideal histogram:

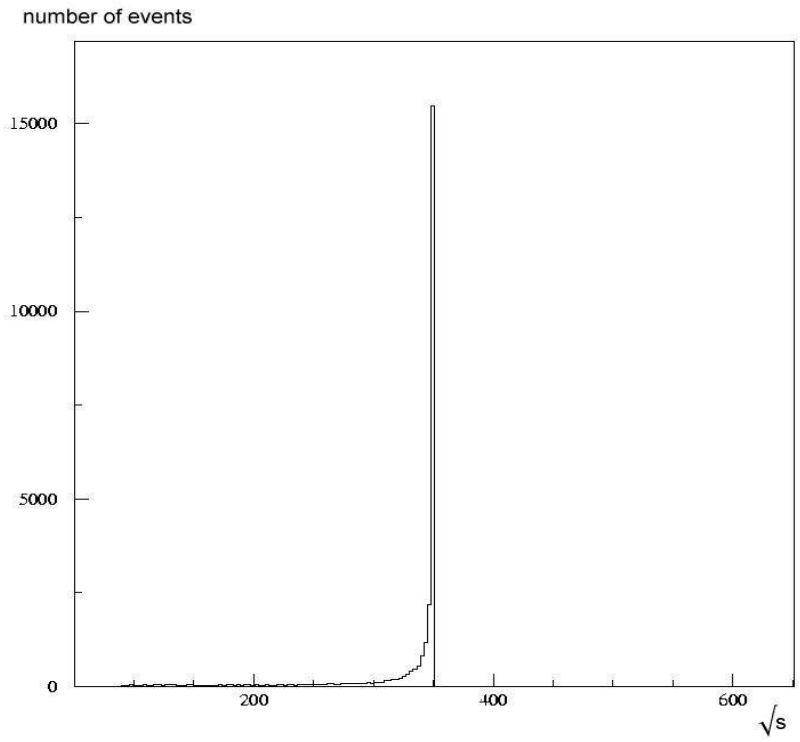

Fig. 6: *Calculated invariant energy $\sqrt{s}$ using $\sqrt{s'}$*

A sharp peak at 350 GeV shows that equation (8) is working well. The tail to the left is due to emission of more than one photon of sizeable energy – while formula (8) would require exactly one photon to compute the exact energy. This is due to initial and final state radiation (ISR)(FSR). Most of these photons are of low energy and do not result in a big error.

Using equation (8) all emitted photons are treated as one (fig. (7)).

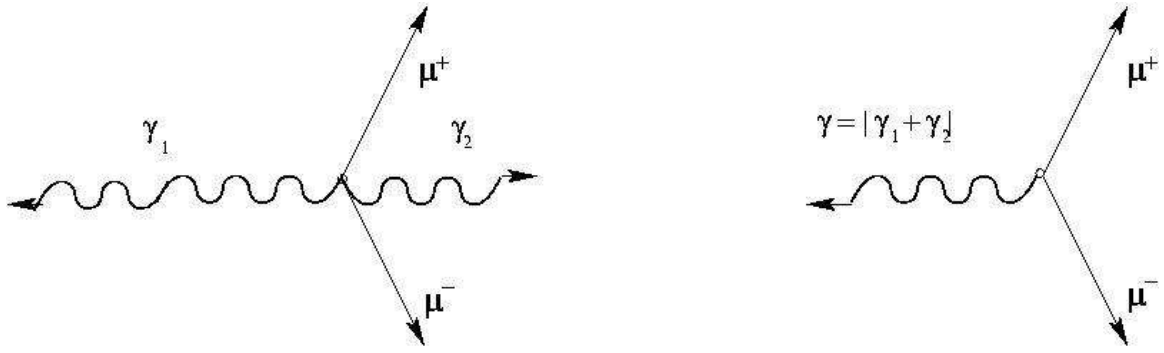

Fig. 7: *More than two photons are treated as one by eq. (8) of chapter II part 2, thus a lower energy is calculated*

Since photons have no rest mass there is no error as long as the photons are emitted in the same direction. If several photons are emitted in different directions the transverse photon momenta subtract and the angles of the muons become larger. If then equation (8) is used a lower center of mass energy is calculated. Since most photons are emitted along the accelerator axis formula (8) works very well.

If a real experiment is performed √s' would have to be measured by a detector. The calibration of this detector is correlated with the calibration of the magnet spectrometer. But our method is used for the calibration of the magnet spectrometer so we should not make use of the center of mass energies of the muons. (see chapter II part 1).
One takes events with an intermediate Z^0 state and uses m_z instead of √s' (see chapter II part 2). Thus from now on equation (9) of Chapter II part 2 is used. A cut at 91 GeV (the Z^0 mass) is applied. Only events in an interval from 86 GeV to 96 GeV are kept.
We assume that the photon is not detected. To use equation (9) we need the angles the muons make with the emitted photon. But in most events the photon is emitted along the accelerator axis. So the angles the muons make with the accelerator axis can be used as approximation.
Making these changes one arrives at the following histogram:

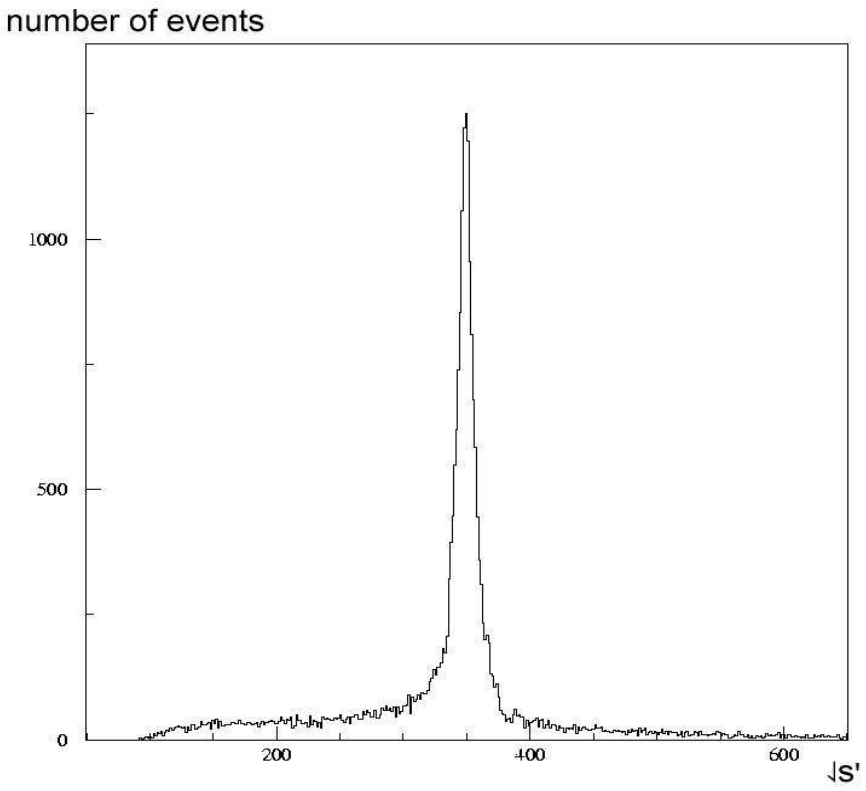

Fig. 8: *Calculated invariant energy √s using m_z*

The peak became a little broader and on the left and right there is a tail due to the use of m_z for all events instead of the true value $\sqrt{s'}$. The left tail is a little higher due to emission of 2 or more photons.
10 100 fb^{-1} Monte Carlo samples were generated at 350 GeV and two 1000 fb^{-1} Monte Carlo samples at 349 GeV and 350 GeV to use the Monte Carlo fit method explained in Chapter II part 3. The fit yielded 349.99 GeV as mean invariant energy and an error of 0.046 GeV. 100 fb^{-1} corresponds to roughly 230,000 events. To check the linearity assumption of the method 10 100 fb^{-1} samples at 350 GeV, 349.5 GeV and 349 GeV were fitted by 3000 fb^{-1} samples at 349 GeV and 350 GeV. If the linearity assumption holds errors and possible shifts should be the same. From the table one sees that a possible shift is well below the statistical errors.

simulated center of mass energy [GeV]	***mean center of mass energy from fitting [GeV]***	***mean error of fit [GeV]***
350	349.99	0.046
349.5	349.50	0.046
349	348.99	0.046

Table 1: *Fit on different samples in the range 349 GeV to 350 GeV to check the linearity assumption of the fit method*

3. Inclusion of beamstrahlung:

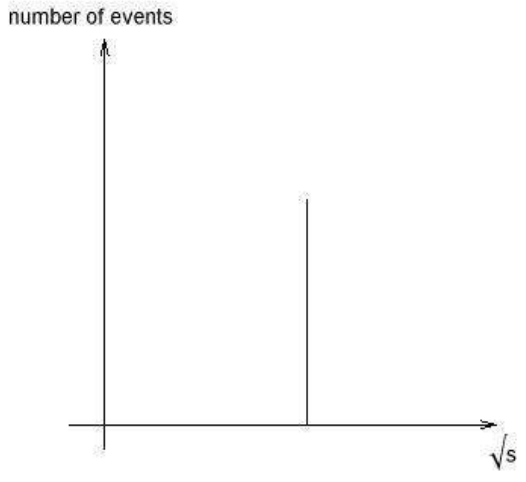

Fig 9: *Schematic view of the original energy distribution of the beam (a delta function)*

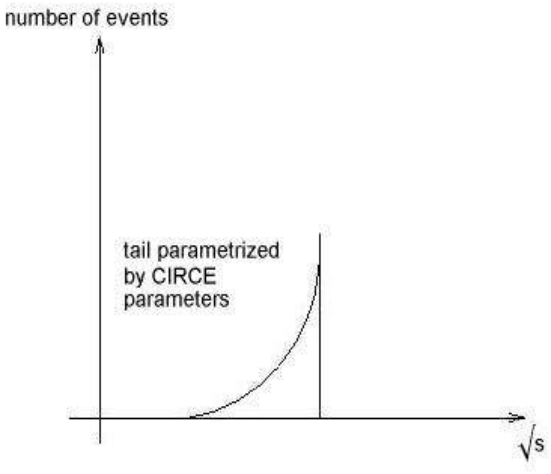

Fig 10: *After CIRCE is applied some particles have a smaller energy*

The electrons and positrons are exposed to coherent electromagnetic fields from the approaching positron/electron bunches. This leads to the emission of photons which are called beamstrahlung. Beamstrahlung is simulated by the package CIRCE [10] which simply assigns a lower energy to the electrons and positrons using a random number generator. The distribution of the energies for TESLA is taken from a function whose parameters are obtained fitting the output of full simulations of beamstrahlung, which would take too much computer time to run.
The distribution used is:

$$f(x)=a_0\,\delta(1-x)+a_1\,x^{a_2}(1-x)^{a_3}$$

where $x=\frac{\sqrt{s'}}{\sqrt{s}}$. In the Ansatz of CIRCE it is assumed that both beams (electrons and positrons) have the same amount of beamstrahlung and that there is no correlation between the beamstrahlung of the two beams. The four parameters have for TESLA the values a_0=0.5274, a_2=13.895 and a_3=-0.6314. The fourth parameter a_1 is given by the normalization condition of a probability distribution $\int f(x)\,dx=1$. Fig. 11 shows the effect of beamstrahlung on the $\sqrt{s'}$ spectrum above 250 GeV (before any cuts are applied):

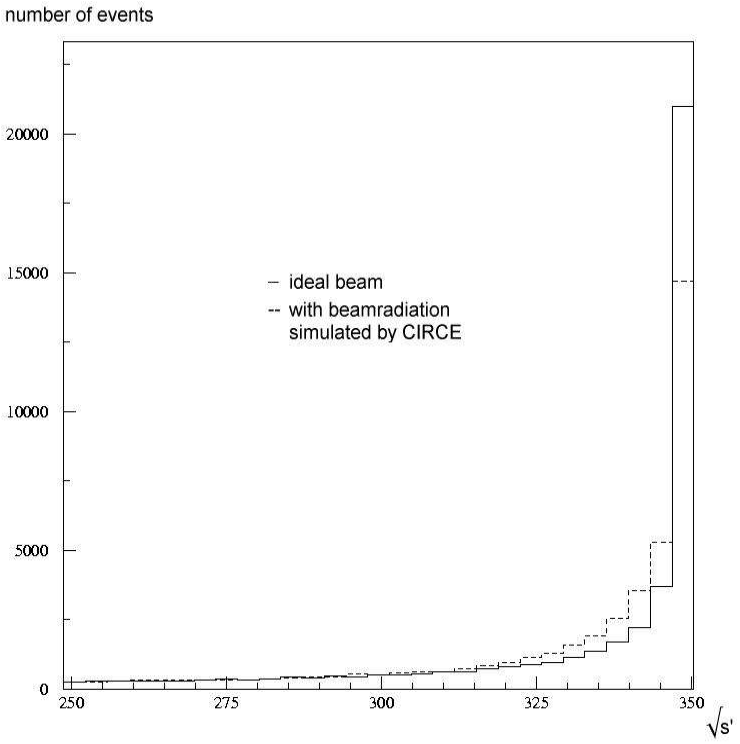

Fig. 11: *Change of the spectrum due to inclusion of beamstrahlung*

Again 10 100 fb^{-1} samples were generated at 350 GeV, two samples of 1000 fb^{-1} at 349 and 350 GeV, through fitting a mean invariant energy of 349.95 GeV and an error of 0.053 GeV was obtained. Compared with the error of the last step the statistical error increased by 7 MeV.

4. Inclusion of 7° cut:

Since the detector can not discern a muon from other particles below 7 degree around the accelerator axis, events generated by PYTHIA where one of the muons is below 7 degree have to be excluded. 10 100 fb^{-1} samples at 350 GeV were generated, two 1000 fb^{-1} Monte Carlo samples at 349 and 350 GeV, the mean invariant energy was 349.96 GeV and the error was 0.050 GeV. Thus the error decreases by 3 MeV because of the 7° cut. The events which are cut are events where the muons have low angles. The enhancement in the error could be due to statistics in these events introduced by larger errors in the calculation of the κ_γ factor for low angles (see chapter II part 2 eq. (6)).

In Fig. 12 one can see the events skipped by the 7° cut:

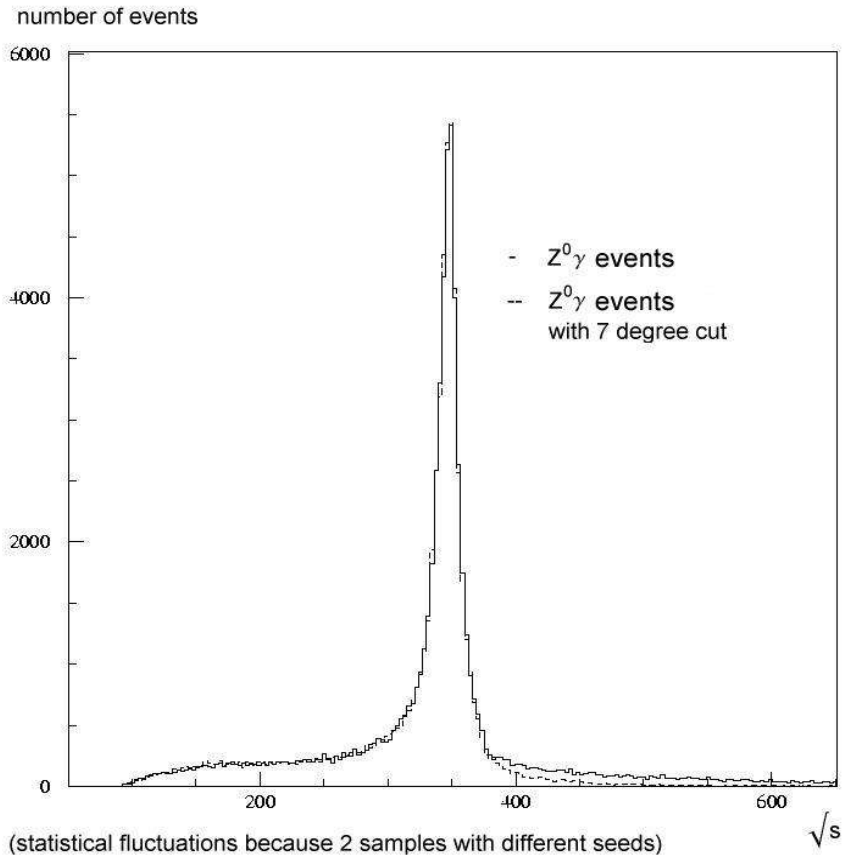

Fig. 12: *Change in energy spectrum due to 7° cut*

5. Inclusion of $Z^0e^+e^-$ background:

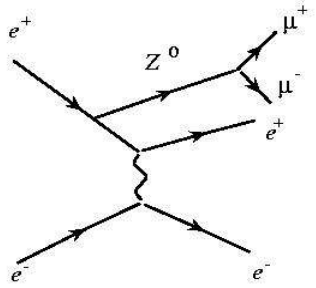

Fig. 13: *The process* $e^+e^- \rightarrow Z\, e^+e^- \rightarrow \mu^+\mu^- e^+e^-$

Consider the process $e^+e^- \rightarrow Z^0\, e^+e^- \rightarrow \mu^+\mu^- e^+e^-$. If the positron and the electron in the final state are below 7 degree and thus cannot be detected the final state of the process looks like the final state of our ideal $e^+e^- \rightarrow Z^0 / \gamma^* \rightarrow \mu^+\mu^-\gamma$ process. So this process has to be included in the simulation. The 100 fb^{-1} correspond now to ~230,000 Z^0 / γ^* events and to ~75,000 $Z^0\, e^+e^-$ events, thus ~305,000 events were generated.
Generating 10 100 fb^{-1} MC samples at 350 GeV and two samples with 1000 fb^{-1} at 349 and 350 GeV, results in a mean invariant energy of 349.98 and an error of 0.048 GeV. This is because $Z^0\, e^+e^-$ has similar kinematics as Z^0 / γ^* and like the Z^0 / γ^* process a small peak around 350 GeV, enhancing the original peak (See fig. 14):

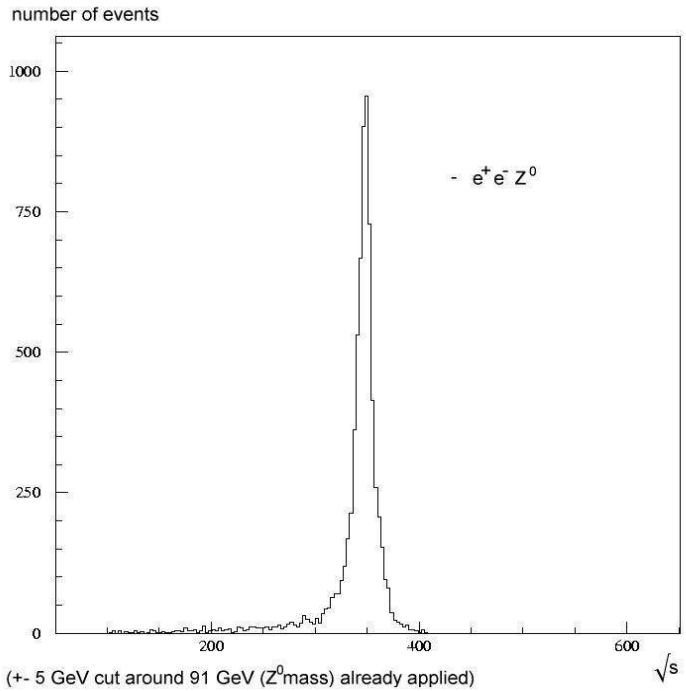

Fig. 14: *$Z^0\, e^+e^-$ events and calculated $\sqrt{s}$ using them. Notice the smaller eventnumber in comparision to fig. 8*

6. Inclusion of $e^+e^-\gamma\gamma$ background:

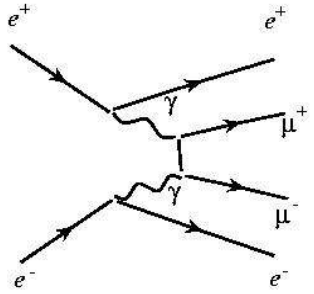

Fig. 15: *The process* $e^+e^- \rightarrow e^+e^- \gamma\gamma \rightarrow \mu^+\mu^- e^+e^-$

For the process $e^+e^- \rightarrow e^+e^- \gamma\gamma \rightarrow \mu^+\mu^- e^+e^-$, similarly to the $Z^0e^+e^-$ background the final state positron and electron could also be below 7 degree and thus go by undetected, so in this case there are no means to discern the process from $e^+e^- \rightarrow Z^0 / \gamma^* \rightarrow \mu^+\mu^-\gamma$.
Including it in the simulation, the 100 fb^{-1} correspond now to ~305,000 Z^0 / γ^* and $Z^0\, e^+e^-$ events, in addition ~1,837,000 $e^+e^- \gamma\gamma$ events, so ~2,142,000 events were generated.
The enormous number of $e^+e^- \gamma\gamma$ events is reduced to ~9000 events by the 5 GeV cut around the Z^0 peak (91 GeV) and the 7° cut around the accelerator axis (See Fig . 16):

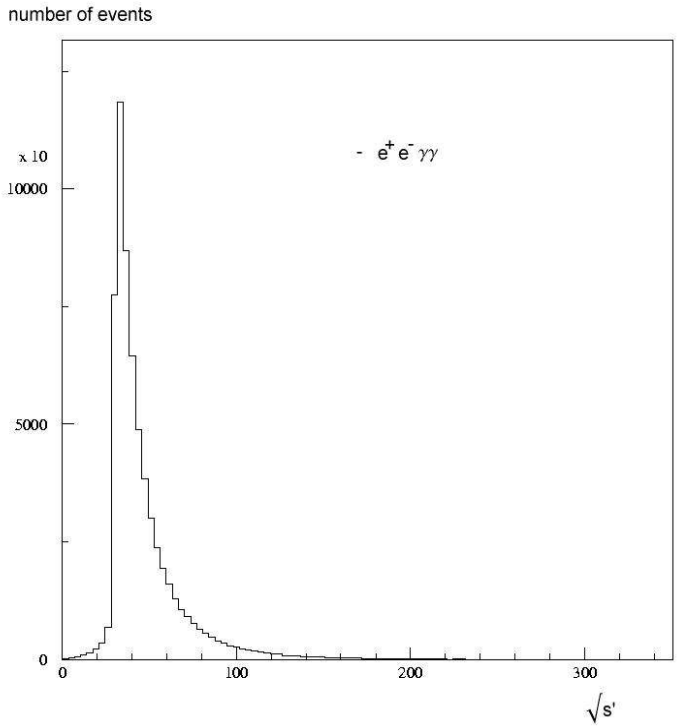

Fig. 16: *$e^+e^- \gamma\gamma$ background before 91 GeV and κ_γ cuts are applied (events below 30 GeV were not generated to save computing time)*

Furthermore a cut to κ_γ (defined in equation (6) of chapter II part 2) was applied: all events above $\kappa_\gamma = 0.95$ were dismissed. This reduced the $e^+e^- \gamma\gamma$ events again to ~6000, which can be seen nicely in Fig. 17:

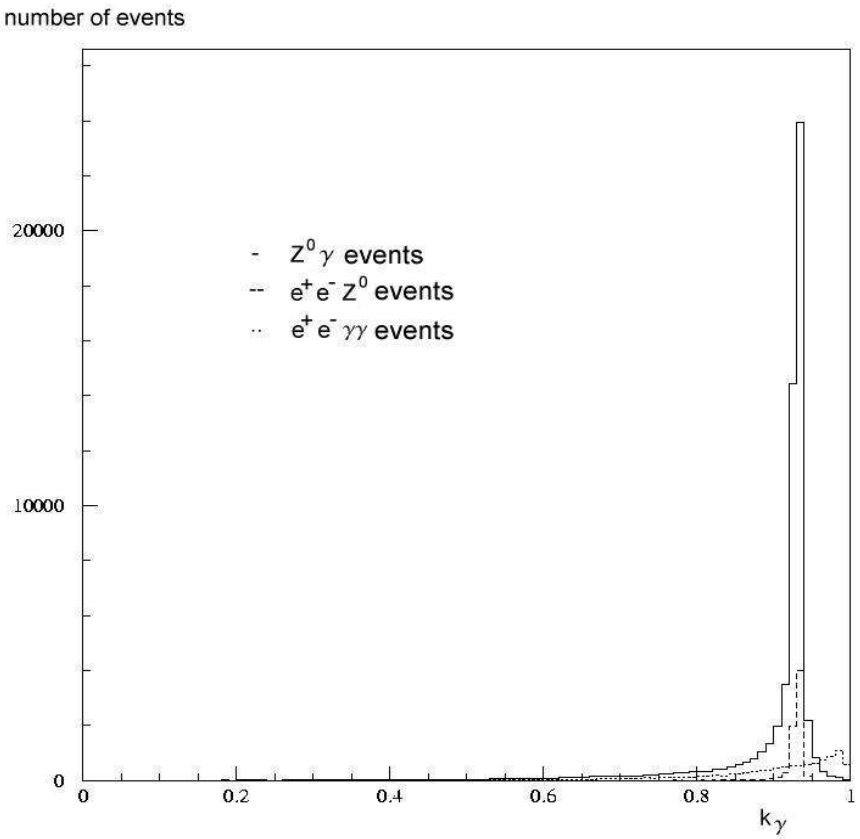

Fig. 17: *Above $\kappa_\gamma = 0.95$ are about 1/3 of the $e^+e^- \gamma\gamma$ events*

10 100 fb^{-1} samples at 350 GeV and two 1000 fb^{-1} samples at 349 and 350 GeV were generated. The mean invariant energy was 349.94 and the error was 0.047 GeV. This change in error should be due to statistical fluctuations.

7. Use of the direction of detected photons:

In the real experiment the detector has several limitations (See chapter II part 4).
Above 7° around the accelerator axis the emitted photons will be detected, while between 3° and 7° one cannot discern photons and electrons/positrons and below 3° nothing is detected.
One can take the direction of photons in account to a certain extent, and calculate the axes the muons make with the emitted photon of the highest energy.
To do this one compares the energy of the photons above 7° with each other, with the energy of photons/electrons/positrons between 3° and 7° and with the rest energy which should have escaped below 3°.
You can calculate this rest energy approximately using the (uncalibrated) measured energy of the beam and subtracting the detected muon and photon/electron/positron energy above 3°. This is only very approximate but enough to discern in which direction the highest energy photon/electron/positron was emitted.
Calculating the new muon angles in this way yields a mean invariant energy of 349.91 GeV and an error of 0.045 GeV. The error in the last step was 47 MeV so it was reduced by taking the direction of the photons into account.
As before 10 100 fb^{-1} samples were generated at 350 GeV, two samples with 1000 fb^{-1} at 349 GeV and 350 GeV.

8. Inclusion of Z^0Z^0/W^+W^- background:

In the process $e^+e^- \rightarrow Z^0Z^0 \rightarrow \mu^+\mu^- \nu \bar{\nu}$, if a real experiment is performed the neutrinos will not be detected at all by the particle detector. So the final state is indistinguishable from the final state of the $e^+e^- \rightarrow Z^0 / \gamma^* \rightarrow \mu^+\mu^- \gamma$ process.
The same applies to the process $e^+e^- \rightarrow W^+ W^- \rightarrow \mu^+ \nu \mu^- \bar{\nu}$.
Generating 100 fb^{-1} samples results in additional ~1163 Z^0Z^0 events and ~ 15602 $W^+ W^-$ events. By the 5 GeV cut around the Z^0 peak the $W^+ W^-$ events are reduced to about 500, so the Z^0Z^0 and $W^+ W^-$ background should not have any effect. (See fig. 18 and fig. 19)
The fit yielded a mean invariant energy of 349.95 GeV and an error of 0.044 GeV.
10 100 fb^{-1} and two 1000 fb^{-1} samples were used (at 350 GeV, 349 GeV and 350 GeV).

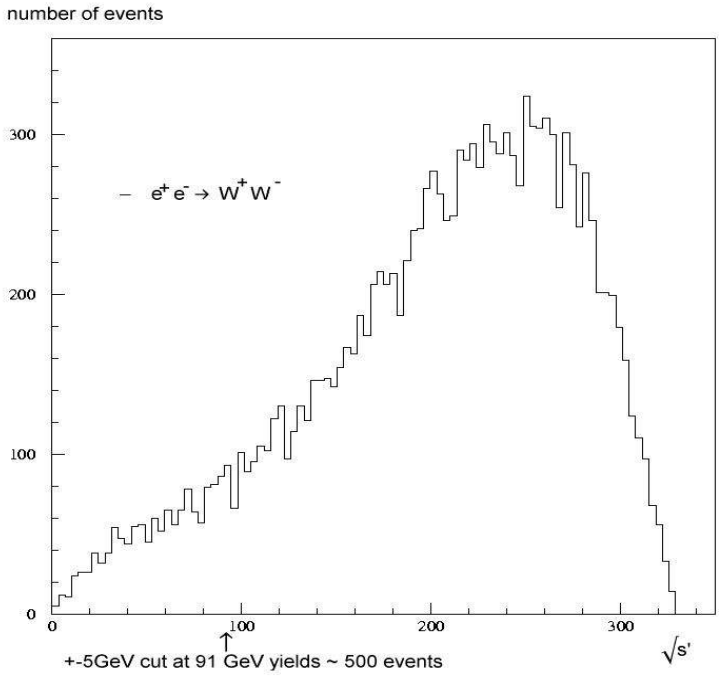

Fit 18: *W^+ W^- events reduced by 5 GeV cut around 91 GeV to around 500 events*

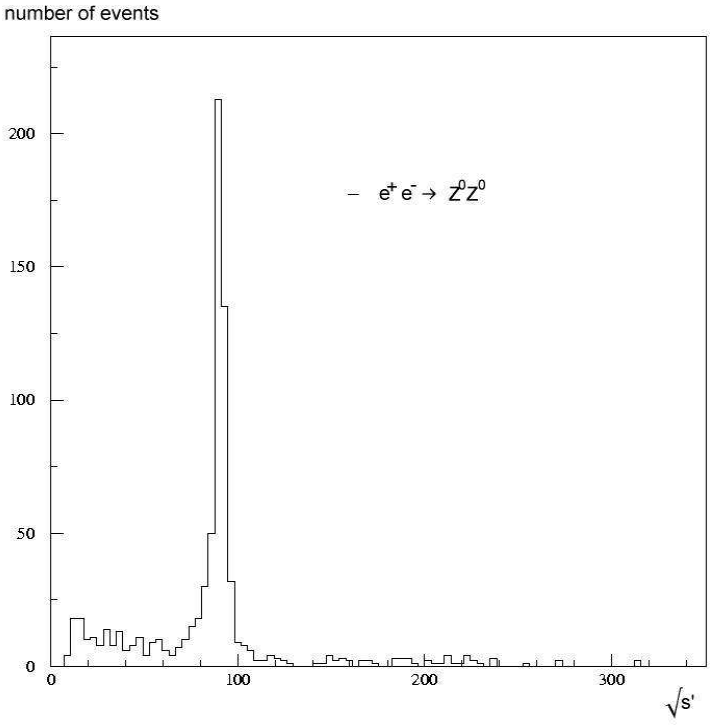

Fit 19: *Z^0Z^0 events reduced by 5 GeV cut around 91 GeV to around 600 events*

9. Using a gaussian shaped energy distribution:

Not single electrons and positrons are accelerated but whole bunches. It is assumed that the electrons/positrons in these bunches will have a gaussian energy distribution at TESLA as suggested by simulations of TESLA [1]. A gaussian distribution of the beam energy was implemented simply by using a gaussian random number generator to assign variations from the nominal CM energy. The variance of the gaussian distribution used was $\sigma = 2 / 1000$, from the fit a mean invariant energy of 350.02 GeV and an error of 0.047 GeV was obtained. Since this is the final sample which simulates all important features of the real data the statistical error of the fit of this sample gives an estimation of the precision the method will have when a real experiment is performed at TESLA. In addition it will be used to study systematic errors. To make the statistical and the systematic error estimates more reliable two 3000 fb^{-1} samples have been used to fit the 10 100 fb^{-1} samples.
Again the linearity of the fit method was checked by performing fits on several samples in the range 349 GeV to 350 GeV. 10 100 fb^{-1} samples were fitted by 3000 fb^{-1} samples. The shifts stay below the statistical error of the fit (see table 2). So the linearity assumption is valid.

simulated center of mass energy [GeV]	***mean center of mass energy from fitting [GeV]***	***mean error of fit [GeV]***
350	350.02	0.047
349.5	349.49	0.047
349	349	0.047

Table 2: *Possible shifts of the fit method stay below the statistical error for samples in the range 349 GeV to 350 GeV*

10. Summary

A Monte Carlo sample was created which takes into account the major background processes, several detector complications as the 7 degree cut and the detection of the photons, the beamstrahlung and an energy distribution. The error in determining the center of mass energy of the final sample is 47 MeV at a luminosity of 100 fb^{-1} . This makes an estimation of running time of the accelerator to achieve a certain precision of the statistical error possible.
The sometimes large deviations of the mean center of mass energies are due to statistical fluctuations in the Monte Carlo samples used to perform the fit on the data. The last Monte Carlo sample which includes all complications has been fit with samples of 3000 fb^{-1} size to make the center of mass energy obtained by the fit reliable.

	luminosity ***[fb^{-1}]***	***simulated center of mass energy*** ***[GeV]***	***mean center of mass energy from fitting*** ***[GeV]***	***mean error of fit*** ***[GeV]***
ideal beam	100	350	349.99	0.046
inclusion of beamstrahlung	100	350	349.95	0.053
incl. of 7° cut	100	350	349.96	0.050
incl. of Ze^+e^- bg.	100	350	349.98	0.048
inclusion of $e^+e^-\gamma\gamma$ backg.	100	350	349.94	0.047
inclusion of the photon direction	100	350	349.91	0.045
inclusion of Z^0Z^0 and W^+W^- backg.	100	350	349.95	0.044
inclusion of a gaussian energy distribution	100	350	350.02	0.047

Table 3: *Behavior of the statistical error during creation of the basic Monte Carlo sample (in each step one more complication is added)*

IV. Monte Carlo samples at different CM energies

To study the behavior of the statistical error of the method at different energies Monte Carlo samples were created at 250 GeV, 350 GeV, 500 GeV, 750 GeV and 1000 GeV. These Monte Carlo samples include all complications as in the final Monte Carlo sample of chapter III.

1. Monte Carlo sample at 250 GeV

At 250 GeV, two 3000 fb^{-1} samples were used to fit 10 100 fb^{-1} samples and an invariant energy of 250.00 GeV and an error of 0.028 GeV resulted.

2. Monte Carlo sample at 350 GeV

At 350 GeV, using 3000 fb^{-1} samples to fit 10 100 fb^{-1} samples, the fit yields an invariant energy of 350.02 GeV and an error of 0.047 GeV.

3. Monte Carlo sample at 500 GeV

At 500 GeV, 3000 fb^{-1} samples to fit 10 100 fb^{-1} samples, one finds an invariant energy of 499.98 GeV and an error of 0.091 GeV.

4. Monte Carlo sample at 750 GeV

At 750 GeV, 3000 fb^{-1} samples to fit 10 100 fb^{-1} samples, an invariant energy of 749.95 GeV and an error of 0.181 GeV were obtained.

5. Monte Carlo sample at 1000 GeV

Since the invariant energy of the beam is much farther away from the Z^0 peak than in the 350 GeV or 250 GeV case fewer events get accepted by the 5 GeV cut around 91 GeV. This results in larger statistical fluctuations in the two Monte Carlo samples used to fit the third one. The size of the samples used to perform the fit was increased to 9000 fb^{-1}. At 1000 GeV, using 9000 fb^{-1} samples to fit 10 100 fb^{-1} samples, one finds an invariant energy of 999.81 GeV and an error of 0.331 GeV.

6. Summary

If one assumes a quadratic relation the statistical error follows the equation:

$$E[MeV] = 8.8027\,MeV - 0.0026\frac{MeV}{GeV}\sqrt{s} + 0.0003\frac{MeV}{GeV^2}s$$

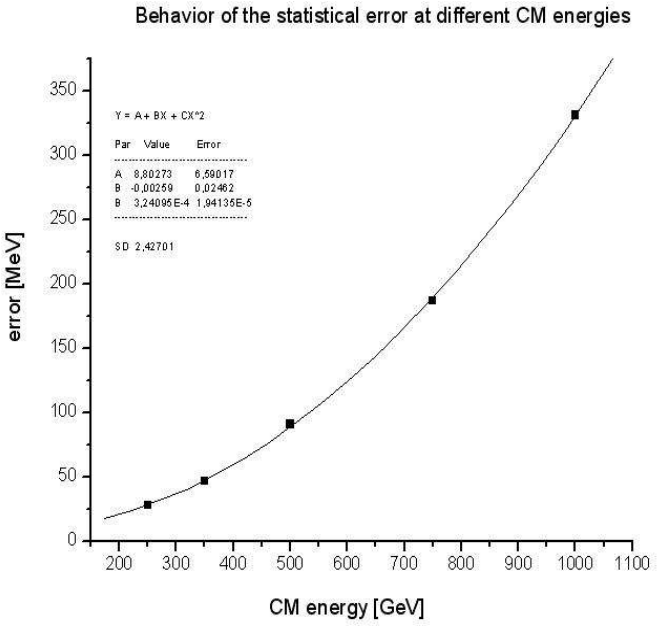

Fig 20: *Quadratic fit of the errors*

*S*ince the statistical error goes like $\frac{1}{\sqrt{(N)}}$ the first possible cause for the quadratic behavior to look at is the number of events of the signal process. Three cuts have been applied so far, the 5 GeV cut around 91 GeV in chapter III. part 2, the κ_γ cut in chapter III part 7 and the 7° cut from chapter III part 5. After these cuts are applied the signal shows a roughly exponential decay with rising center of mass energy (see fig. 21).
The $Z^0e^+e^-$ background has similar kinematics to the Z^0/γ^* process and therefore lowers the statistical error (see chapter III part 5). This process rises with larger center of mass energy (fig. 22) as does the $e^+e^-\gamma\gamma$ background process (fig. 23).

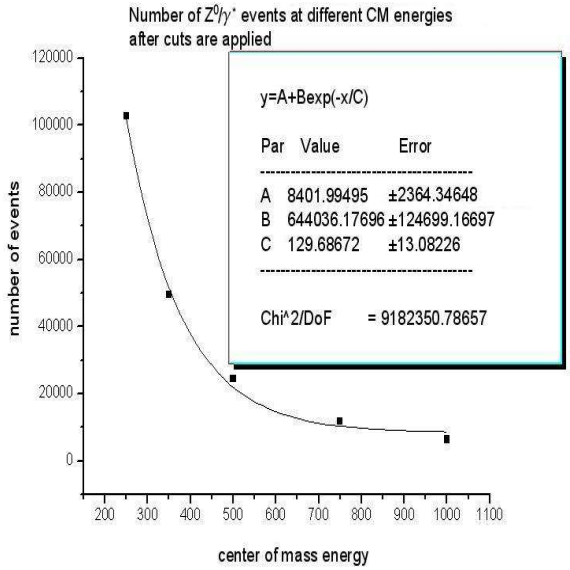

Fig. 21: *Number of events of the Z^0/γ^* process at different center of mass energies*

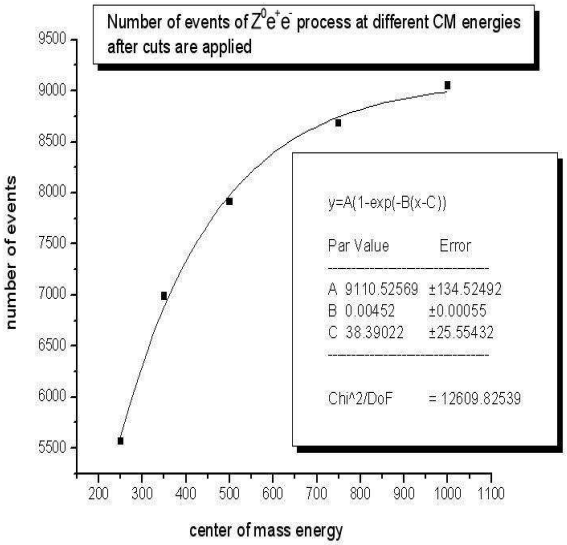

Fig. 22: *Number of events of Ze^+e^- background at diff. CM energies*

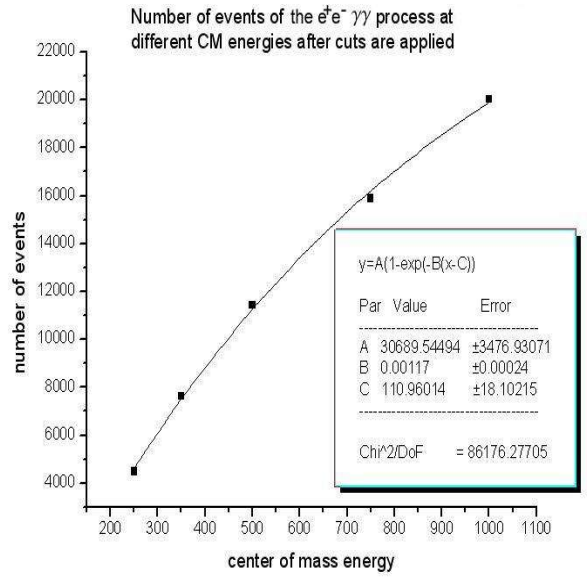

Fig. 23: *Number of events of $e^+e^-\gamma\gamma$ background at different CM energies*

The combination of these behaviors do not result in a quadratic behavior but there are a number of other effects which are hard to quantify:

1.
Emission of more than one high energy photon gets more likely for higher center of mass

energies. The method makes the assumption of exactly one high energy photon emitted (see chapter III part 2).

2.
The effect of beamstrahlung gets larger with higher center of mass energy.

3.
One expects that the variance of the gaussian energy distribution (chapter III part 9) gets larger with larger center of mass energies. In the Monte Carlo simulation a variance of 2/1000 of the center of mass energy was assumed.

4.
There could also be statistics introduced on generator level

	luminosity ***[fb^{-1}]***	***simulated center of mass energy*** ***[GeV]***	***mean center of mass energy from fitting*** ***[GeV]***	***mean error of fit*** ***[GeV]***
MC sample at 250 GeV	100	250	250	0.028
MC sample at 350 GeV	100	350	350.02	0.047
MC sample at 500 GeV	100	500	499.98	0.091
MC sample at 750 GeV	100	750	749.95	0.181
MC sample at 1000 GeV	100	1000	999.81	0.331

Table 4: *The statistical error of the method at different CM energies*

V. Systematic errors due to background

There are uncertainties in the modeling of background processes. Either because of shortcomings in the theoretical description of the processes or because approaches which are more imprecise are used in the simulation to save computing time.
The fit method (chapter II part 3) makes use of Monte Carlo samples to fit the data. Uncertainties in the MC samples produce shifts when the fit is performed and therefore systematic errors result.
There are several possibilities to get an estimation of these systematic errors. For example one could compare results from different Monte Carlo generators to see what differences in background the approaches used in the generators yield. These differences are then assumed as error in the amount of background. For the background processes considered here a 10% uncertainty in background is realistic (see [6]). A fit is performed on a sample with varied background to see possible shifts in the determination of the center of mass energy. To get shifts which clearly are not due to statistics one assumes larger uncertainties and scales them afterwards down to 10%.
The basic Monte Carlo samples after the Z^0Z^0 and the W^+W^- background was included were used (see chapter III part 8) but to the 10 100 fb^{-1} samples additional background events were added. The shifts from the reference invariant energy of 349.95 GeV of the original samples give an estimation of the error.

1. 20% additional Ze^+e^- background:

20% more Ze^+e^- at 100 fb^{-1} translated to 8000 additional Ze^+e^- events (before cuts are applied). They were just added to the already existing 100 fb^{-1} histograms and the existing 1000 fb^{-1} samples were used to fit them, thus obtaining an estimate of possible shifts in energy and error if a 20% too low background is assumed. The fit yielded as invariant energy 349.95 GeV and as error 0.045 GeV, so the error changed marginally. No shift is observed thus no systematic error is assigned.

2. 20% fewer Ze^+e^- background:

Now the 8000 additional Ze^+e^- events were subtracted from the already existing 100 fb^{-1} histograms and the existing 1000 fb^{-1} samples were used for fitting. This simulates a 20% too high background. The invariant energy was 349.95 GeV and the error was 0.043 GeV, so there is only a small change in the error. Since there is no shift no systematic error results.

3. 30% additional $e^+e^-\gamma\gamma$ background:

30% additional $e^+e^-\gamma\gamma$ events meant about 56,700 more events before cuts are applied. As before, they were added to the existing 100 fb^{-1} histograms and the existing 1000 fb^{-1} samples were used for the fit procedure. This corresponds to the assumption of a 30% too low background. The resulting invariant energy was 349.94 GeV and the error was 0.044 GeV. Scaling to a 10 % uncertainty in the $e^+e^-\gamma\gamma$ background results in a shift of 3 MeV. The systematic error is then 3 MeV.

4. 30% fewer $e^+e^-\gamma\gamma$ background:

The 56,700 $e^+e^-\gamma\gamma$ were subtracted from the 100 fb^{-1} histograms using the 1000 fb^{-1} samples for fitting. The invariant energy was 349.96 GeV and the error was 0.045 GeV. The systematic error of 10% fewer background is 3 MeV.

5. Summary

20% and 30% are already quite large uncertainties in background and the shifts observed do still stay under the statistical error, more realistic are around 10% and the scaling to this value resulted in negligible systematic errors.

	luminosity [fb^{-1}]	***simulated center of mass energy [GeV]***	***mean center of mass energy from fitting [GeV]***	***mean error of fit [GeV]***	***scaled systematic error [MeV]***
reference is ZZ/WW included:	100	350	349.95	0.044	
+20% Ze^+e^- background	100	350	349.95	0.045	0
-20% Ze^+e^- background	100	350	349.95	0.043	0
+30% $e^+e^-\gamma\gamma$	100	350	349.94	0.044	3
-30% $e^+e^-\gamma\gamma$	100	350	349.96	0.045	3

Table 5: *Systematic errors due to background*

VI. Systematic errors from other sources

There are several more sources of systematic errors, mainly uncertainties of different parameters used to create the Monte Carlo samples. To get an estimation of those errors one creates 10 100 fb^{-1} samples with a variation in the parameter in question corresponding to its assumed error. Then the basic 3000 fb^{-1} Monte Carlo samples of chapter III part 9 are used to fit these 10 samples. A shift in the mean invariant energy from 350 GeV gives an estimation of the systematic errors of the method.

1. Shape of the energy distribution

Since the electrons and positrons are accelerated as bunches they do not have a certain well defined energy but follow a distribution of energies. As simulations show the distribution will be approximately gaussian at TESLA [1]. In the creation of the Monte Carlo samples a gaussian distribution was assumed for TESLA. To see possible errors due to another shape of the energy distribution one fits 10 100 fb^{-1} samples with a rectangular distribution.

10 samples with a rectangular energy distribution of same variance as the gaussian distribution of chapter III part 9 were generated. For a rectangular distribution $s=2/\sqrt{12}\ L$, where L is half of the length of the rectangular. Therefore $L=\sqrt{12}*1/1000$ to have the same variance as the gaussian distribution.
This yielded a mean invariant energy of 350.01 GeV and an error of 0.047 GeV. Therefore the change in shape from gaussian to rectangular results in a shift of only 0.01 GeV, and a systematic error of 10 MeV is assigned.

2. Variance of the gaussian energy distribution

There will also be uncertainties in the variance of the gaussian distribution of TESLA. To simulate this one fits 10 100 fb^{-1} samples with larger σ.

10 samples with a broader gaussian distribution of $\sigma = 10 / 1000$ were generated. The fit resulted in a mean invariant energy of 349.98 GeV and the error was 0.048 GeV. Thus a difference/uncertainty in the variance of about 8/1000 results in a 0.02 GeV shift. An uncertainty in the variance of about 1/1000 is realistic [1]. Scaling to 1/1000 uncertainty the systematic error is < 3 MeV.

3. Error due to uncertainty in the aspect ratio of the detector:

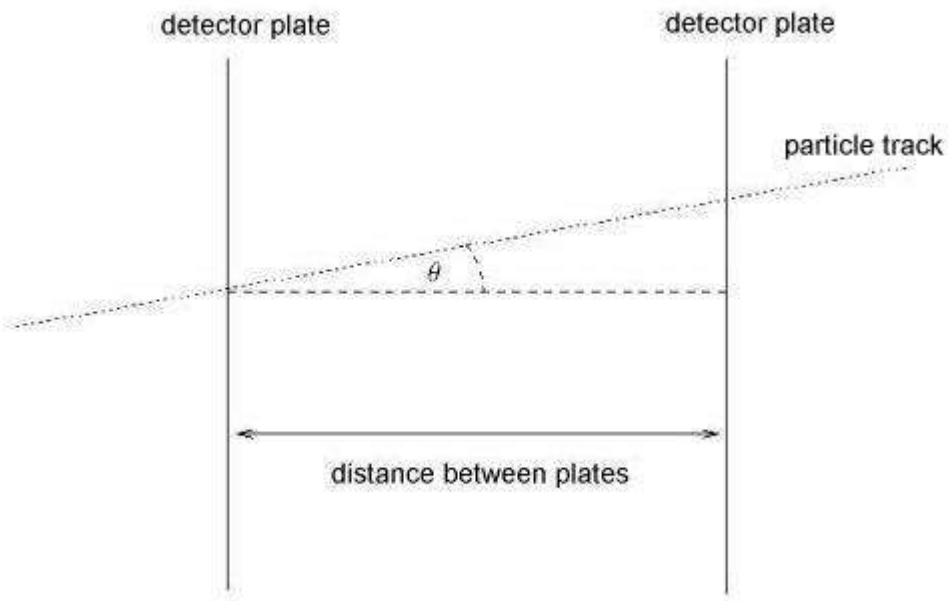

Fig 24: *A particle track through 2 detector plates*

The angles of particles in a detector are determined by tracking them through several detector plates and dividing possible deviations in the points where they pass the plates through the distance between the plates (see fig. 24). If this distance is not known exactly a shift in the angles of the particles results. The same applies if the ratio of the two distances, the distance between the plates and the deviation of subsequent passing points is not known exactly. The ratio of x to y length of the detector at LEP was only known up to 0.0005 [2] thus producing a shift in the angles measured.
A similar error for TESLA is assumed here. To simulate this 10 100 fb^{-1} samples were created with artificially changed angles so as if the length of the detector along the accelerator axis was 1.0005 of the usual length. Angles near 45˚ are changed most (~0.014˚), angles near 10˚ or 80˚ are changed ~0.0048˚. The change is symmetric around 45˚.
The fit yielded a mean invariant energy of 350.16 GeV and an error of 0.047 GeV. This results in 160 MeV systematic error.

4. Error due to uncertainity in parameters of CIRCE:

The inclusion of beamstrahlung via CIRCE as mentioned in chapter III part 3 is errorenous because the parameters CIRCE uses to simulate beamstrahlung are obtained

through fitting the output of full simulations of beamstrahlung. An estimation of these errors can be found for example in [4]. Generating 10 100 fb^{-1} samples with a change in parameter a_0 of 0.012, the mean invariant energy was 350.04 and the error was 0.047. A change in parameter a_2 of 0.24 resulted in 350.00 GeV and 0.047 GeV and a change in a_3 of 0.0048 yields 349.97 GeV and 0.047 GeV. The errors mentioned in [4] are $\Delta a_0 = 0.012$, $\Delta a_2 = 0.12$ and $\Delta a_3 = 0.0024$, respectively. The results show that a variation of a_0 yields the biggest shift of 0.04 GeV, while the variation of a_2 and a_3 results in shifts of 0.0 GeV and 0.03 GeV. Thus a systematic error of 40 MeV for a_0 and 15 MeV for a_3 is obtained. The changes in the spectrum of the Monte Carlo sample due to variation of the circe parameters is shown in figures 25 to 27. They are in accordance to the parameterizing function which was introduced in chapter III part 3:

$$f(x) = a_0 \delta(1-x) + a_1 x^{a_2} (1-x)^{a_3}$$

where $x = \frac{\sqrt{s'}}{\sqrt{s}} < 1$ and parameter values as given in chapter III part 3.

In fig. 25 a_0 was lowered by 0.4 which lowered the number of events at nominal center of mass energy. Since a_1 is calculated through the normalization condition (see chapter III part 3) the number of events in all bins are raised proportionally.
In fig. 26 a_2 was lowered by 10 which makes the beamstrahlung tail steeper and lowers all bins proportionally.
In fig. 27 a_3 was lowered by 0.4 which makes the tail less steep and raises all bins.

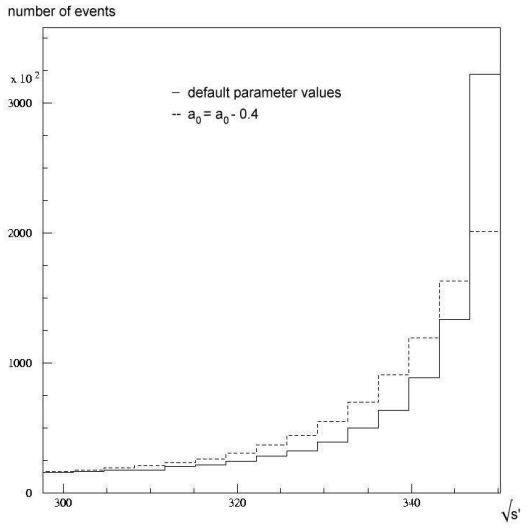

Fig. 25: *Lowering a_0 lowers the number of events at default center of mass energy*

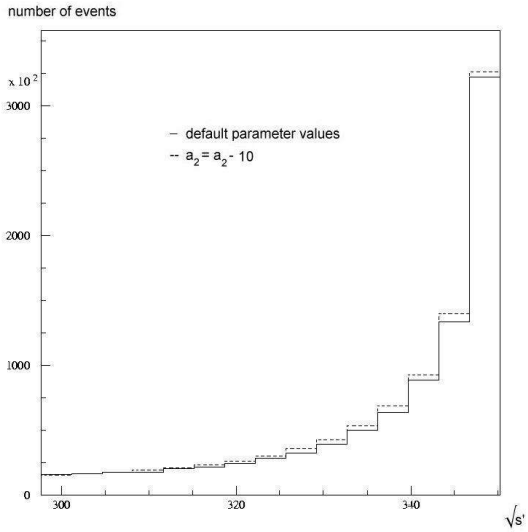

Fig 26: *Lowering a_2 makes the tail steeper* (since $x=\frac{\sqrt{s'}}{\sqrt{s}}<1$)

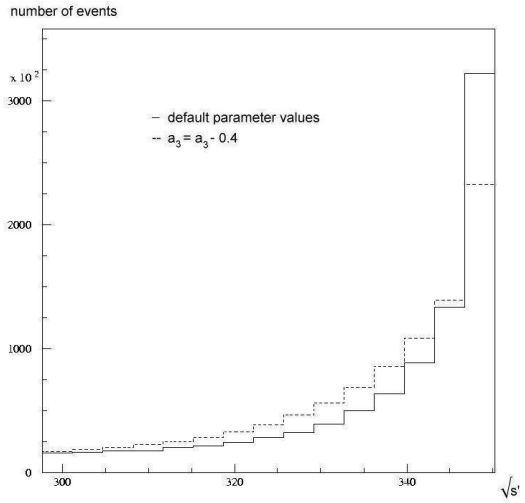

Fig. 27: *Lowering a_3 makes the tail less steep*

(since $x=\frac{\sqrt{s'}}{\sqrt{s}}<1$ and $a_3<0$)

5. Summary

The uncertainties in the aspect ratio and in the CIRCE parameter a_0 and possibly a_3 are the major sources of systematic errors. Especially the aspect error should be kept below the level of LEP. The systematic error in using a rectangular energy distribution could also be due to statistics since no scaling was possible in this case.

	luminosity ***[fb^{-1}]***	***simulated center of mass energy*** ***[GeV]***	***mean center of mass energy from fitting*** ***[GeV]***	***mean error of fit*** ***[GeV]***	***scaled systematic error [MeV]***
gaussian energy distribution with bigger σ	100	350	349.98	0.048	< 3
rectangular energy distribution with same σ	100	350	350.01	0.047	10
aspect error	100	350	350.16	0.047	160
$a_0 = a_0 + 0.012$	100	350	350.04	0.047	+40
$a_2 = a_2 + 0.24$	100	350	350.00	0.047	0
$a_3 = a_3 + 0.0048$	100	350	349.97	0.047	-15

Table 6: S*ystematic errors due to energy distribution, detector aspect ratio and CIRCE parameters*

VII. Overview of the Results

1.
The kinematic formulas for calculating $\sqrt{s}$ were derived in chapter II part 2. They were subsequently modified to apply them to the method of radiative return events.

2.
A method to fit the Monte Carlo data samples was found in chapter II part 3.

3.
The Monte Carlo samples which were obtained in chapter III hopefully represent very closely the experimental data of TESLA. They are needed to use the fitting method described in chapter II part 3 to fit real experimental data.

4.
The statistical error of the fit of the Monte Carlo samples obtained in chapter III part 9 is 47 MeV for a 100 fb^{-1} sample. This allows an estimation of running time (luminosity) which will be needed to achieve a certain precision concerning the statistical error of the method.

5.
The behavior of the statistical error of the method at different center of mass energies is given by the quadratic fit of chapter IV part 6:

$$E[MeV] = 8.8027\,MeV - 0.0026\frac{MeV}{GeV}\sqrt{s} + 0.0003\frac{MeV}{GeV^2}s$$

6.
Possible shifts from the true center of mass energies can be estimated by the systematic errors obtained in chapter V and VI. It was shown that the aspect error and the uncertainty in a_0 and a_3 of the CIRCE parameters are the major systematic errors.

7.
The other systematic errors (background processes, shape of the energy distribution) were shown to be negligible.

error source	*systematic error*
+10% Ze^+e^- background	0 MeV
+10% $e^+e^-\gamma\gamma$	3 MeV
gaussian energy distribution with $\sigma=\sigma(1+1/1000)$	< 3 MeV
rectangular energy distribution with same σ	10 MeV
aspect error 1/1.0005	160 MeV
$a_0 = a_0 + 0.012$	+40 MeV
$a_2 = a_2 + 0.12$	0 MeV
$a_3 = a_3 + 0.0024$	-15 MeV

Table 7: S*ummary of the systematic errors*

VIII. Future development

1.
The statistical error alone will at 350 GeV (using 100 fb^{-1}) be 47 MeV which is well above the 35 MeV demanded by [5]. To reduce it under 35 MeV at least 200 fb^{-1} have to be used (see chapter III part 10).

2.
The next step should be to concentrate on reducing the systematic error introduced by the aspect error (see chapter VI part 3).

3.
The systematic errors which result from the CIRCE parametrization (see chapter VI part 4) have to be studied in more detail.
In the present study correlations between the CIRCE parameters have not been taken into account.
In addition CIRCE does not take into account beamstrahlung correlations between the electron and positron beams. So there will be additional systematic errors due to errorenous simulation of beamstrahlung.

4.
Other processes which have three body final states should be included, for example $e^+e^-\gamma$, $\tau^+\tau^-\gamma$ etc. to lower the statistical error of the method for a given luminosity.

5.
There are different models to simulate Initial State Radiation. There will be systematic errors due to imprecise simulation of ISR.

6.
It is left for investigation whether there are error sources not considered and included up to now.

IX. References

[1] *Technical Design Report*, DESY 1001 - 011, ECFA 2001 – 209, Tesla Report 2001 – 23, March 2001

[2] The DELPHI Collaboration, K. Hamilton, P.J. Holt, G. Morton, G Myatt, M Nikolenko, *Preliminary determination of e_{beam} at LEP2 using radiative 2 fermion events in DELPHI*, DELPHI 2002 – 084 CONF 618, 1. July 2002

[3] Helge Todt, *Determination of the beam energy at TESLA using radiative dimuon events*, Student Reports: www-zeuthen.desy.de/students/2003/

[4] K. Mönig, *Measurement of the differential luminosity using Bhabha events in the forward tracking region at TESLA*, LC – PHSM – 2000 – 60 TESLA, 29. December 2000

[5] V.N. Duginov, et al., *The TESLA beam energy spectrometer*, submitted as LC note, to be published November 2004

[6] The OPAL Collaboration, *Determination of the LEP beam energy using radiative fermion pair events*, OPAL physics note PN520, 30. June 2003

[7] The L3 Collaboration, *Measurement of the Z boson mass using $e^+e^- \rightarrow Z^0/\gamma^*$ events at centre of mass energies above the Z pole*, CERN – EP / 2003 – 074, November 18. 2003

[8] DELPHI Collaboration, Jim Libby, Geoff Morton, *Measurement of the 1997 beam energy using $e^+e^- \rightarrow \mu^+\mu^-\gamma$*, DELPHI 98 – 152 phys 796, 31. August 1998

[9] T. Sjöstrand, P Edén, C. Friberg, L. Lönnblad, G. Miu, S. Mrenna and E. Norrbin, *PYTHIA 6.154,* Computer Phys. Commun. 135 (2001) 238, LU TP 00-30, hep- ph/0010017

[10] T. Ohl, *CIRCE version 2.0: Beam spectra for simulating linear collider and photon collider physics, 2002, WUE-ITP-2002-006*

[11] *Undulator based production of polarized positrons*, 7. June 2003, SLAC- PROPOSAL-E-166